Desalination and Water Treatment
www.deswater.com
doi: 10.5004/dwt.2021.26976

218 (2021) 401–408
April

Synergistic effect of adsorption and Fenton-like oxidation processes for Methylene blue removal using Na-P1 zeolite prepared from pumice

Vicky Prajaputra[a,b], Zaenal Abidin[b,*], Sri Budiarti[c], Dyah Tjahyandari Suryaningtyas[d]

[a]*Study Program of Natural Resources and Environmental Management, Bogor Agricultural University, Bogor 16144, West Java, Indonesia*
[b]*Department of Chemistry, Bogor Agricultural University, Bogor 16680, West Java, Indonesia, email: abidinzed@apps.ipb.ac.id (Z. Abidin)*
[c]*Department of Biology, Bogor Agricultural University, Bogor 16680, West Java, Indonesia*
[d]*Department of Soil and Land Resources, Bogor Agricultural University, Bogor 16680, West Java, Indonesia*

Received 21 March 2020; Accepted 21 December 2020

ABSTRACT

The most problem in the combination of adsorption and Fenton oxidation processes is the low ability of sorbents to degrade organic pollutants. Therefore, the sorbents need to be modified by adding metal salt compounds, especially those containing iron. In this study, we investigated the use of natural pumice to prepare zeolites with high catalytic properties without adding iron sources. Pumice-based zeolite was prepared through simple hydrothermal alkaline treatment and used to remove Methylene blue (MB) from aqueous solution. The characterization results confirmed that the mineral phase of pumice was successfully transformed to GIS-NaP1 zeolite. The maximum value of adsorption capacity increased highly from 7.80 to 35.33 mg g^{-1} after the treatment process. Adsorption isotherm showed a better fit to the Langmuir model with a high correlation coefficient value (R^2 = 0.999) compared to the Freundlich model (R^2 = 0.882). This means the interaction between zeolite and MB followed the assumption of monolayer adsorption on homogeneous surfaces. Interestingly, the synergistic effect of adsorption and Fenton oxidation processes enhanced the ability of zeolite to remove MB with efficiency from 60.92% to 99.99%. Furthermore, zeolite can also be reused several times without reducing its performance significantly after regeneration.

Keywords: Catalytic; Environmental sciences; Equilibrium study; Materials; Methylene blue

1. Introduction

Dyes have been recognized as useful organic compounds used in many industries, such as pharmaceuticals, plastic, art, paper, cosmetics, food, and textiles [1]. Although most dyes are produced from different plant sources, they can also be synthesized via a chemical reaction. One of the synthetic dyes is Methylene blue (MB) which has first been used by Paul Ehrlich as an antimalarial drug in the year 1891. Afterward, MB was replaced by chloroquine and other synthetic drugs from its derivatives without staining properties. In textile industries, MB is widely used as coloring agents because of their stability to light exposure and inexpensive [2]. Sometimes, dyes are unable to be bonded strongly with fabric fibers and will be lost during the washing process into the water. It has been reported that approximately 700,000 tonnes of dye wastewater are discharged every year to the environment with concentrations ranging from 10–200 mg L^{-1} [3,4]. The contamination of dyes in water becomes a significant issue for the environmental ecosystem due to its toxicity and mostly non-biodegradable, which finally leads to human health problems [5].

* Corresponding author.

Several commercial methods have been applied for managing organic pollutants in water, such as electrocoagulation [6], ozone oxidation [7], ultrafiltration [8], bioremediation [9], and adsorption [10]. Among the mentioned methods, adsorption is well-known as an effective and affordable method due to its flexibility, ease to handle, and economical safe without wasting a lot of solvents [11]. Several low-cost adsorbents had been investigated, such as volcanic ash soil [12], kaolinite [13], bentonite [14], fly ash [15], and zeolite [16]. In recent years, many studies used zeolites as the most potential adsorbent and catalyst carriers because of their unique adsorption properties and high cation exchange capacities [17,18]. Metal salt compounds containing Fe or Cu play an important role to improve zeolite catalytic properties by ion-exchange procedures or hydrothermal synthesis method [19–21]. According to Gonzalez-Olmos et al. [22], the use of Fe-zeolite composite for degrading organic compounds through Fenton reaction was significantly affected by the presence of Fe contents to generate reactive oxidant species. Yet, the addition of iron salt compounds, such as iron sulfate or ammonium iron citrate solutions as Fe ion sources for preparing Fe-zeolite composites needs an extra cost and difficult to apply on a large scale.

In the present study, natural pumice was chosen as an adsorbent candidate due to its several characteristics. Based on related references, the pumice thermal stability reaches approximately 900°C with a specific surface area of 28 $m^2\ g^{-1}$ [23,24]. It has a high porosity of up to 85% [25]. The availability of pumice, especially in Indonesia, is abundant because of its specific location in the "pacific ring of fire" region. Also, the main components of pumice are SiO_2, Al_2O_3, and Fe_2O_3 [26], which can be potentially used to prepare zeolite with high catalytic properties without adding any metal salt compounds. Here, the integration of adsorption and Fenton oxidation processes using pumice-based zeolite was studied for the removal of MB in an aqueous solution.

2. Materials and methods

2.1. Materials preparation

The natural pumice was obtained from the Suwung area, Bali, Indonesia with a specific coordinate location at 8°43'14.0"S 115°13"16.0"E (–8.720560, 115.221117). The collected pumice was dried for a day to remove the content of water. Then, dried-pumice was ground and filtered by using a standard molecular sieve (100 mesh) to reduce its particle size. All chemical substances, such as MB dye ($C_{16}H_{18}ClN_3S$), hydrogen peroxide (H_2O_2), and sodium hydroxide or caustic soda (NaOH), were purchased from Nacalai Tesque lnc., (Kyoto, Japan) with high-quality grade. A stock of MB solution (1,000 mg L^{-1}) was prepared using distilled water.

2.2. Hydrothermal synthesis of GIS-NaP1 zeolite

The synthesis of pumice-based zeolite was carried out by the simple hydrothermal alkaline treatment, following the previous report [27]. Briefly, 10 g of pumice was dissolved within 80 mL of sodium hydroxide solution (2.5 mol L^{-1}) under the stirring conditions for 30 min. The mixture was heated in a sealed-polypropylene bottle at 100°C for a day to initiate the formation of zeolite crystals. Zeolite was then separated, rinsed until neutral pH, and dried again at 100°C for a half day. The functional groups of pumice and synthesized products were identified by Fourier-transform infrared spectroscopy (FTIR) spectra using a Perkin Elmer Spectrum One FTIR spectrometer (Massachusetts, USA), which recorded in the range of 4,000–500 cm^{-1}. The mineralogical analysis was determined by X-ray diffraction (XRD) using a X-ray diffractometer (Bruker D8, Texas, USA) ranging from 5°–50° using Cu Kα radiation at 40 kV and 30 mA (scan rate of 2°/min).

2.3. Dye adsorption process

The adsorption process was performed within various MB concentrations in the range of 25–300 mg L^{-1}. About 50 mg of adsorbents was added into several centrifuge tubes containing 10 mL of MB solution with different initial concentrations and shaken for a minute. The adsorption processes were operated at ambient temperature for one day, in which the uptake capacity of adsorbents was measured by determining MB concentrations before and after the adsorption process using a Spectronic 20D+ spectrometer. The quantity of adsorbed MB (q_e in mg g^{-1}) was calculated by using Eq. (1).

$$q_e = \frac{\left(C_0 - C_e\right)V}{m} \tag{1}$$

where q_e is the uptake capacity in equilibrium condition (mg g^{-1}); C_0 and C_e are the initial and equilibrium MB concentrations in mg L^{-1}, respectively; m is the amount of adsorbents (g) and V is the total volume of MB solution (L).

2.4. Fenton oxidation process

The Fenton oxidation process was carried out at a concentration of MB 300 mg L^{-1}, which was adsorbed by adsorbents. After 24 h of adsorption time, 0.5 mL of hydrogen peroxide solution (12.8 mol L^{-1}) was added dropwise and shaken for a minute. The Fenton experiment was evaluated at room temperature for 6, 12 and 24 h. After that, the mixture was centrifuged for 15 min and the supernatant was separated quickly. The final MB concentration was then measured by using a Spectronic 20D+ spectrometer. From Eq. (2) the degradation efficiency (%D) was calculated.

$$\%D = \frac{C_0 - C_e}{C_0} \times 100 \tag{2}$$

2.5. Reusability of adsorbents

The most important criteria of adsorbents to minimize the cost in the adsorption process is their stability and reusability during reaction [28]. The reusability of pumice and treated-pumice was investigated by dropping 10 mL of MB solution (300 mg L^{-1}) into 50 mg of adsorbents. The mixture was shaken for a minute and left at room temperature for 1 d. Then, 0.5 mL of hydrogen peroxide solution (12.8 mol L^{-1}) was added immediately. After 1 d, the mixture was separated by using a centrifuge

and the final MB concentration was measured. The adsorbent was then carefully rinsed with deionized water and dried at 100°C for 12 h. This process was repeated several times using the regenerated adsorbent. The adsorbent stability before and after regeneration was determined by FTIR spectra.

3. Results and discussion

3.1. Materials characterization

Natural pumice compositions was determined from X-ray fluorescence (XRF) analysis (Table 1) [26]. The infrared spectra comparison of pumice before and after alkaline treatment in the range of 500 to 4,000 cm^{-1} are shown in Fig. 1. This comparison was carried out to ensure that the formation of zeolite frameworks has occurred. Before alkaline treatment, the spectra of pumice were well-defined by four different peaks at wavenumbers of 720, 1,000, 1,650 and 3,475 cm^{-1}. The detected peaks around 1,000 and 720 cm^{-1} were individually assigned as characteristic peaks for the symmetric stretching vibration of Si–O–Si in the functional group of $(SiO_4)^{2-}$ and the bending vibration of Si–O bond, respectively. Furthermore, other absorption bands corresponded to the adsorbed water molecule and hydrogen bonding in the pumice structure, in which the peak at 1,650 cm^{-1} contributes to the bending vibration of H–O–H bond and the broadening band at 3,475 cm^{-1} to the asymmetric stretching vibration of O–H bond [29]. Overall, the pumice spectra showed strong bonding vibrations between silicon and hydroxyl groups in the structure. On the other hand, after alkaline treatment of pumice, several new peaks appeared in the fingerprint region at 745, 680 and 595 cm^{-1}. Vibration bands at 745 and 680 cm^{-1} contributed to the internal tetrahedron symmetric stretching vibration and the symmetric stretching of T–O–T bond, respectively, where T refers to Si or Al. The main characteristic of the zeolite spectrum occurred at wavenumber around 595 cm^{-1}, which indicated a double ring vibration in the zeolite framework. Similar results were also reported by Hildebrando et al. [30].

Table 1
Chemical composition of natural pumice

Composition	%
SiO_2	63.45
Al_2O_3	17.24
Fe_2O_3	2.86
TiO_2	0.37
CaO	3.22
P_2O_5	0.21
SrO	0.09
MgO	1.03
K_2O	2.16
SO_3	0.16
Na_2O	2.00
Cl^-	0.30

The XRD patterns of pumice and zeolite are summarized in Fig. 2. As seen, there are significant changes that occurred in mineralogical phases of both materials. The pumice pattern only showed amorphous contents (glassy phase) as the only peak appeared at 2θ degrees between 20° and 30°. A study by Li et al. [29] had reported that the rapid cooling and depressurization of high-temperature volcano lava adversely affected the crystalline content of pumice. In the process, depressurization produced bubbles by reducing the boiling point of the lava. Simultaneous cooling then froze the bubbles in the pumice matrix and reduced the growth of tiny crystals (poor crystallinity). The treated-pumice under alkaline media increased the crystallinity, signed by appearing new characteristic peaks at 2θ degree (d value) = 12.48° (7.08), 17.70° (5.00), 21.65° (4.10), 28.07° (3.17), 33.39° (2.68), 38.02° (2.36), 42.20° (2.13), and 46.02° (1.97). These mineralogical phases were compared to zeolite pure phases from the International Zeolite Association (IZA) and confirmed a high similarity to Na-P1

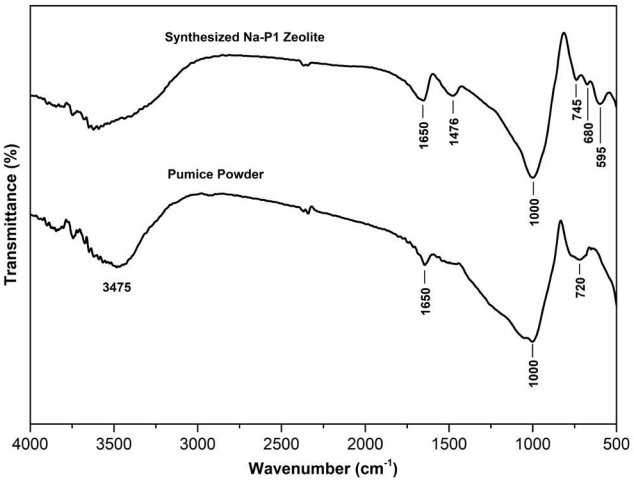

Fig. 1. FTIR spectra of raw pumice and Na-P1 zeolite.

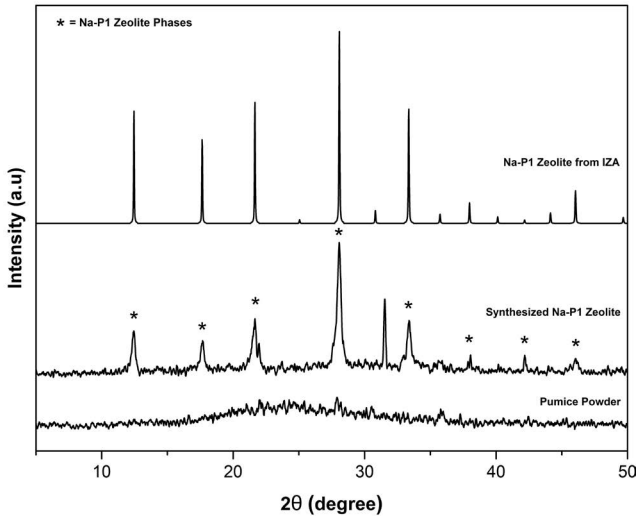

Fig. 2. XRD pattern of pumice and Na-P1 zeolite.

zeolite phases. It can be related to the dissolution or depolymerization of SiO_2 phases, which then caused rearrangement structures to form zeolite frameworks. According to JCPDS data (no. PDF#97-000-9550), Na-P1 zeolite had several characteristic peaks at 2θ degree (*d* value) = 12.46° (7.10), 17.66° (5.02), 21.67° (4.10), 28.10° (3.17), 33.38° (2.68), 38.10° (2.36), 42.20° (2.14), and 46.08° (1.97). In addition, Ismail et al. [31] reported that Na-P1 zeolite contains high silica contents, where the ratio of Si/Al was found to be 3 or greater.

3.2. Equilibrium and adsorption isotherm studies

The adsorption equilibrium provides information about the maximum MB uptake to the sorbent, which was investigated with several initial MB concentrations from 25–300 mg L^{-1}. The initial pH of MB solution determined using a pH meter was found to be 6. The adsorption study used the uptake process as long as 24 h at room temperature to ensure the equilibrium state. Fig. 3a presents the effect of initial MB concentrations on the adsorption ability of pumice and Na-P1 zeolite. The result showed that the pumice adsorption capacity increased from 4.82 to 7.80 mg g^{-1} with increasing the concentration from 25 to 150 mg L^{-1}, respectively. MB is well-known as one of the cationic dyes, which can be ionized in an aqueous solution by forming positive charges. These positive charges allowed pumice to bind with MB molecules because the pumice surface tends to be negative due to the presence of silanol groups. Asgari et al. [32] reported that the pumice surfaces contain permanent negative charges under both acidic and alkaline conditions in the range pH of 2–12. This phenomenon is also supported by Ersoy et al. [23]. Therefore, pumice can be directly used for adsorbing MB molecules, although it has a low adsorption capacity. However, increasing the concentration of MB from 150 to 300 mg L^{-1} decreased the uptake capacity from 7.80 to 7.63 mg L^{-1}, which indicated that the adsorption equilibrium was achieved at 150 mg L^{-1}. In equilibrium condition, the final pH of the MB solution was similar to the initial dye solution (pH = 6).

Pumice exhibited a low adsorption capacity than Na-P1 zeolite. It may be related to the use of pumice without further purification and still contains a lot of impurities. These impurities covered the active side of pumice, thus affected its performance in the adsorption process. However, the treated-pumice with an alkaline solution followed by heating and washing processes had succeeded in reducing impurities and changing the molecular structure of pumice to form a zeolite framework. In the formation of zeolite frameworks, many new silanol groups are formed and directly increased negative charges on zeolite surfaces. Therefore, zeolite was able to reduce MB concentration with a high proportion compared to pumice. Zeolite

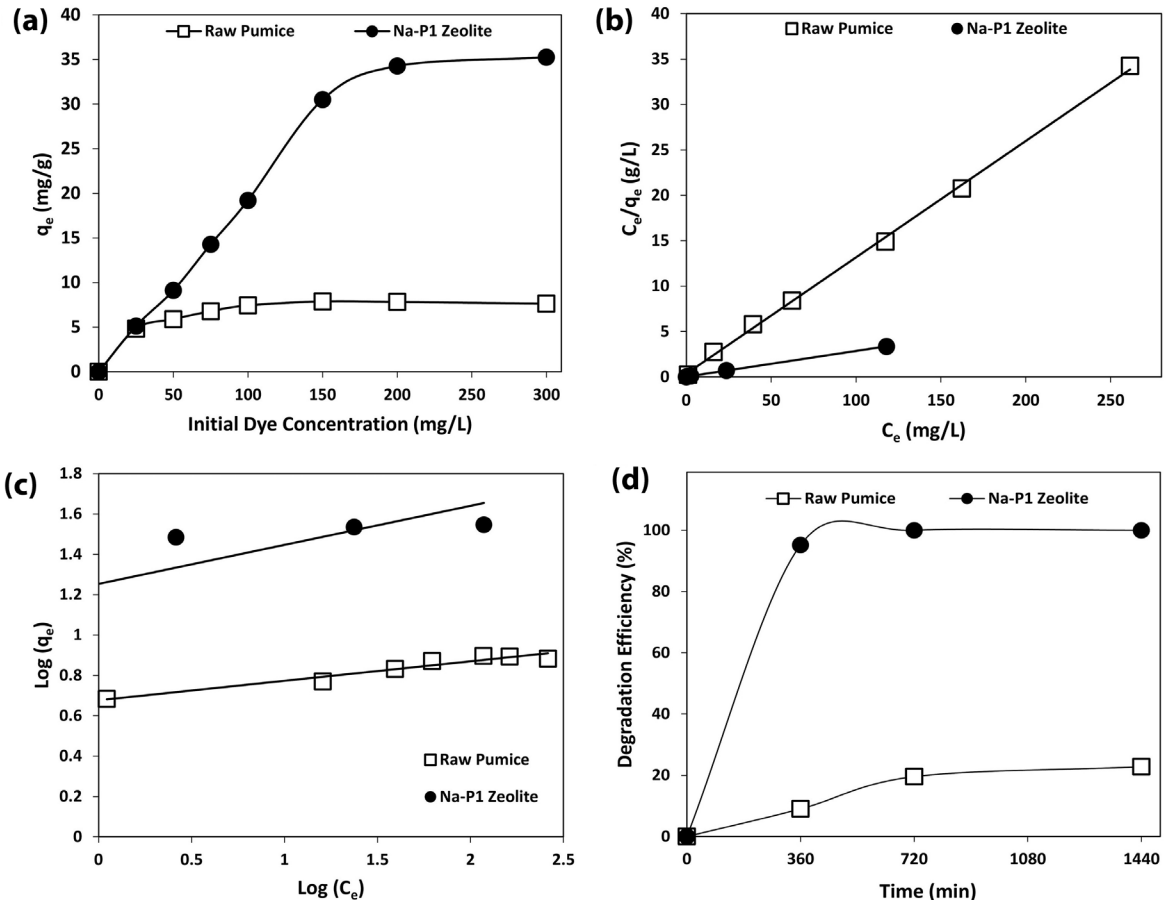

Fig. 3. Study of MB removal.

uptake capacity increased highly from 5.12 to 34.26 mg g^{-1} at MB concentrations of 25–200 mg L^{-1}, respectively. The adsorption rate showed a slight increase with inducing the MB concentration from 200 to 300 mg L^{-1}, in which the adsorption equilibrium was obtained at 300 mg L^{-1} with the uptake capacity of 35.25 mg g^{-1}.

There are two main isotherm models used, namely Langmuir and Freundlich isotherm models. The Langmuir isotherm is the most useful isotherm for both physical and chemical adsorptions model, which indicates homogeneous binding sites for monolayer adsorption, where each of the active sites has equivalent sorption energy [33]. The linear form of the Langmuir isotherm model can be referred to Eq. (3):

$$\frac{C_e}{q_e} = \frac{1}{bq_{\max}} + \frac{C_e}{q_{\max}} \tag{3}$$

where b and $q_{\max}$ are the adsorption equilibrium coefficient (L mg^{-1}) and the adsorption capacity in maximum condition (mg g^{-1}), respectively. Langmuir isotherm model was determined by plotting regression between C_e/q_e vs. C_e for MB adsorption (Fig. 3b). Pumice and zeolite had correlation coefficient values (R^2) of Langmuir isotherm as much as 0.9990 and 0.9999, respectively.

Contrastively, the Freundlich isotherm model assumes that the uptake process occurs on a heterogeneous surface, where the stronger binding site is occupied first and the binding strength decreases as a result of increasing degree of occupation [34]. The regression plotting between C_e/q_e vs. C_e (Fig. 3c) was used in the Freundlich isotherm model to obtain correlation coefficient and other parameter values. The linear form of this model was given by Eq. (4):

$$\log q_e = \log K_f + \frac{1}{n}\log C_e \tag{4}$$

where K_f is Freundlich constant and n is adsorption intensity. The n value can be also used to determine if the uptake process is linear ($n = 1$), physical ($n > 1$) or chemical ($n < 1$) [35]. The correlation coefficient values of Freundlich isotherm using pumice and zeolite were 0.9433 and 0.8821, respectively.

Parameters of Langmuir and Freundlich isotherm models are listed in Table 2. Based on the correlation coefficient values (R^2) of both isotherm models, pumice and zeolite were well-fitted with Langmuir model due to the higher coefficient values compared to the Freundlich model. It means the surface sites of both adsorbents were homogeneous and limited to monolayer coverage, in which the maximum uptake capacities were 7.80 mg g^{-1} for pumice and 35.33 mg g^{-1} for zeolite. The comparison of maximum MB uptake capacity using several adsorbents is listed in Table 3. As shown, NaOH-treated pumice had the higher MB adsorption compared to other low-cost adsorbents such as natural zeolite, fly ash, and kaolin.

3.3. MB degradation and mechanism

The adsorption mechanism of MB molecules onto Na-P1 zeolite had been reported in our previous study [27]. To overcome the weakness of the adsorption method, which only transfers organic pollutants from liquid or gas phases to solid phases, this method was integrated with advanced oxidation processes (AOPs) using a Fenton-like reaction. The presence of iron oxide in samples, especially Fe_2O_3, can be utilized as a trigger for starting the Fenton-like process by adding hydrogen peroxide to generate reactive radicals. The result of MB degradation using pumice and zeolite is presented in Fig. 3d. Pumice had the capability for removing MB molecules even though in low degradation efficiency. It can be related to many impurities in pumice that reduced the adsorption capacity and effected the ability of pumice to degrade MB molecules. Pumice degradation ability increased from 8.99% to 19.53% with increasing contact time from 360 to 720 min. At 1,440 min, the removal efficiency tended to be constant with a percentage of 22.79%. Meanwhile, the ability of Na-P1 zeolite to remove MB molecules increased highly at 360 min with a degradation efficiency of 95.15% and reached 99.9% only at 720 min. Therefore, the adsorption and degradation of MB simultaneously by Na-P1 zeolite is more efficient than a pumice stone.

After the degradation process for 24 h, Na-P1 zeolite was dried and characterized again by FTIR spectroscopy to investigate its stability. The FTIR spectra of MB powder, Na-P1 zeolite, zeolite after MB adsorption, and zeolite after degradation process are displayed in Fig. 4. The spectrum of MB had several vibration peaks, such as the vibration peak of aromatic rings at 1,597 cm^{-1}, the CH_3 symmetrical or asymmetrical vibration at 1,395 cm^{-1} and the C–N stretching vibration at 1,340 cm^{-1}. After adsorption, the spectrum of zeolite showed that MB was adsorbed on zeolite surfaces, which was remarked by the presence of an aromatic ring, $–CH_3$, and C–N vibration peaks. The loss of all mentioned vibration peaks in the zeolite revealed that the MB dye was successfully degraded. Zeolites were considered to have good stability because the spectra of zeolite before adsorption and after the degradation process did not change significantly.

The proposed mechanism of MB degradation is shown in Fig. 5. All of the adsorbed MB molecules are present on the zeolite surface due to the interaction between positive charges of MB and negative charges of zeolite. The presence of iron content, especially Fe_2O_3 as a source of Fe^{3+} in the zeolite framework, reacts with hydrogen peroxide by producing peroxyl radicals ($HO_2^{\bullet}$) and Fe^{2+} as the reduced

Table 2
Parameters of isotherm adsorption model

Model	Parameters	Adsorbent	
		Pumice	Na-P1 zeolite
Langmuir	$q_{\max}$	7.8003	35.3357
	a_L	0.3693	2.7212
	K_L	2.881	96.1538
	R^2	0.999	0.9999
Freundlich	$1/n$	0.0963	0.1933
	K_f	1.9678	3.5033
	R^2	0.9433	0.8821

Table 3
Comparison of maximum MB uptake capacity on several adsorbents

Adsorbents	Maximum uptake capacity (mg g^{-1})	References
Natural zeolite	23.60	Jafari-zare and Habibi-yangjeh [37]
Fly ash	7.07	Janoš et al. [38]
NaOH-treated fly ash	12.64	Woolard et al. [39]
Kaolinite	13.99	Ghosh and Bhattacharyya [40]
NaOH-treated raw kaolin	16.34	Ghosh and Bhattacharyya [40]
Pumice from Bali	7.88	This work
NaOH-treated pumice	35.25	This work

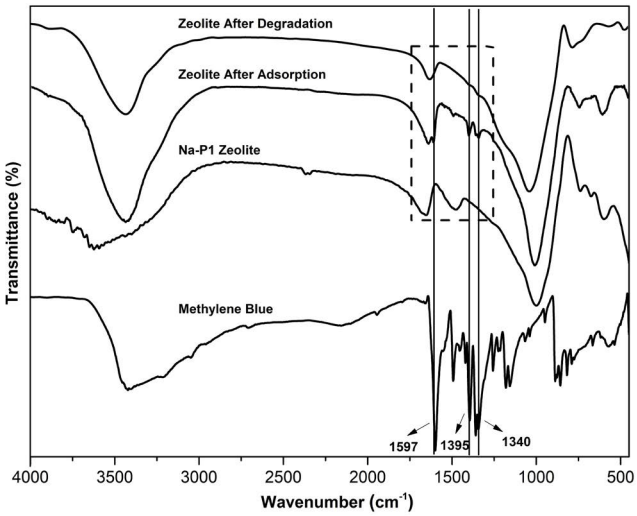

Fig. 4. FTIR spectra of zeolite before and after the treatment process.

form. The reaction between Fe^{2+} and H_2O_2 produces hydroxyl radicals ($OH^{\bullet}$) as a highly reactive oxidant species, that directly attacks MB molecules. The rate of MB degradation depends on the amount of iron content because the more iron content in adsorbents, the faster degradation of dye by the Fenton-like process and vice versa. According to Wang et al. [36], H_2O, CO_2, and other simple organic compounds were found as the final degradation product of MB.

3.4. Reusability of adsorbents

The reusability of pumice and zeolite was performed by stirring 50 mg of adsorbents with 20 mL of MB solution (300 mg L^{-1}) for 24 h. Each replication was conducted by the triple procedure for managing the loss of adsorbent dose during the washing process. The use of Na-P1 zeolite showed a high MB removal efficiency for the investigation of three runs and reached the maximum degradation after 12 h, while the use of pumice presented a low removal efficiency level (Fig. 6). The obtained degradation efficiency values of MB molecule using raw pumices

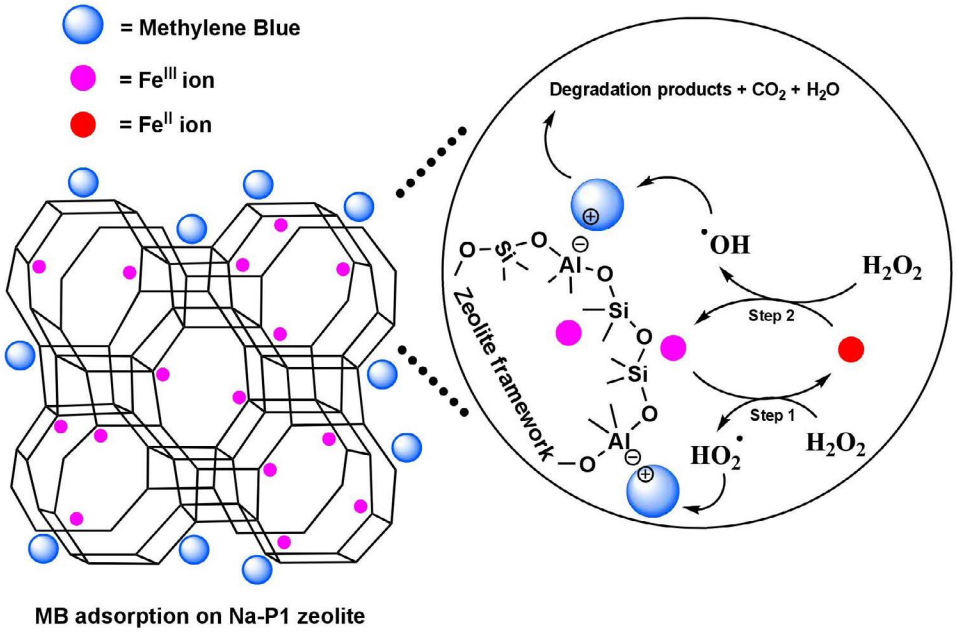

Fig. 5. Proposed mechanism for MB removal on the zeolite surface.

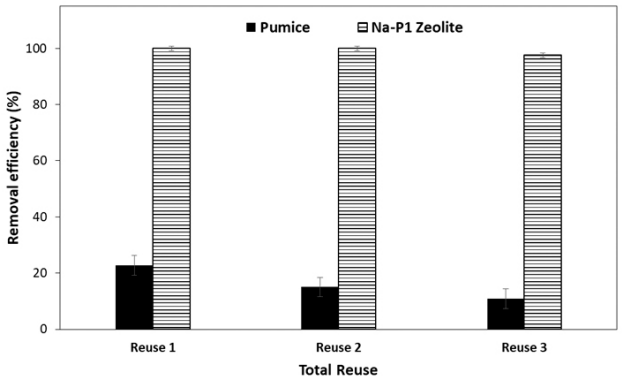

Fig. 6. Reusability of pumice and Na-P1 zeolite for 24 h in several runs.

were 22.79% (reused 1), 20.03% (reused 2), and 10.92% (reused 3) for 24 h. Meanwhile, the degradation efficiency values of Na-P1 zeolite was found to be 99.9% (reused 1), 99.9% (reused 2), and 97.54% (reused 3). This indicates that Na-P1 zeolite was not only had adsorption and degradation abilities for the removal of MB but also can be regenerated to be reused in the other process without reducing its ability significantly.

4. Conclusions

Na-P1 zeolite had been successfully prepared from pumice through a simple hydrothermal route, which was confirmed by using FTIR and XRD analysis results. The equilibrium concentration of MB adsorbed by pumice sample was 150 mg L^{-1} with an adsorption capacity of 7.08 mg g^{-1} (13.40%), while Na-P1 zeolite was able to adsorb MB concentration up to 300 mg L^{-1} with a capacity value of 35.33 mg g^{-1} (60.92%). The adsorption process was fitted to the Langmuir isotherm model for both adsorbents with high correlation coefficient value ($R > 0.99$) than the Freundlich isotherm model. This means the adsorption process followed the assumption of monolayer coverage on homogeneous surfaces. Interestingly, the removal efficiency of MB using zeolite increased highly from 60.92% to 99.9% at a concentration of 300 mg L^{-1} by combining adsorption and Fenton oxidation processes, while the pumice only achieved 22.79% from 13.40%. Furthermore, Na-P1 zeolite can also be reused several times without reducing its efficiency significantly.

Acknowledgments

This research was fully supported by the Ministry of Research, Technology and Higher Education of Indonesia (3/E1/KP.PTNBH/2019). We also deeply thank the Department of Inorganic Chemistry, Faculty of Mathematics and Natural Sciences, IPB University, Indonesia for facilities and equipments.

References

[1] H.B. Mansour, Y. Ayed-Ajmi, R. Mosrati, D. Corroler, D. Barillier, L. Chekir-Ghedira, Acid violet 7 and its biodegradation products induce chromosome aberrations, lipid peroxidation, and cholinesterase inhibition in mouse bone marrow, Environ. Sci. Pollut. Res., 17 (2010) 1371–1378.
[2] K. Elnagar, S. Sanad, A. Mohamed, A. Ramadan, Mechanical properties and stability to light exposure for dyed Egyptian cotton fabrics with natural and synthetic dyes, Polym. Plast. Technol. Eng., 44 (2005) 1269–1279.
[3] T. Robinson, G. McMullan, R. Marchant, P. Nigam, Remediation of dyes in textile effluent: a critical review on current treatment technologies with a proposed alternative, Bioresour. Technol., 77 (2001) 247–255.
[4] A.A. Kadam, A.A. Telke, S.S. Jagtap, S.P. Govindwar, Decolorization of adsorbed textile dyes by developed consortium of *Pseudomonas* sp. SUK1 and *Aspergillus ochraceus* NCIM-1146 under solid state fermentation, J. Hazard. Mater., 189 (2011) 486–494.
[5] M.A. Castro, V. Nogueira, I. Lopes, T. Rocha-Santos, R. Pereira, Evaluation of the potential toxicity of effluents from the textile industry before and after treatment, Appl. Sci., 9 (2019) 3804, https://doi.org/10.3390/app9183804.
[6] A. Suresh, S. Sathish, G.N. kumar, Electrocoagulation of azo dye containing synthetic wastewater using monopolar iron electrodes and the characterization of the sludge, Water Pract. Technol., 14 (2019) 587–597.
[7] S.N. Malik, P.C. Ghosh, A.N. Vaidya, S.N. Mudliar, Catalytic ozone pretreatment of complex textile effluent using Fe^{2+} and zero valent iron nanoparticles, J. Hazard. Mater., 357 (2018) 363–375.
[8] M. Jiang, K. Ye, J. Deng, J. Lin, W. Ye, S. Zhao, B. van der Bruggen, Conventional ultrafiltration as effective strategy for dye/salt fractionation in textile wastewater treatment, Environ. Sci. Technol., 52 (2018) 10698–10708.
[9] C.C. Azubuike, C.B. Chikere, G.C. Okpokwasili, Bioremediation techniques-classification based on site of application: principles, advantages, limitations and prospects, World J. Microbiol. Biotechnol., 32 (2016) 180, https://doi.org/10.1007/s11274-016-2137-x.
[10] A.A. Oyekanmi, A. Ahmad, K. Hossain, M. Rafatullah, Adsorption of Rhodamine B dye from aqueous solution onto acid treated banana peel: response surface methodology, kinetics and isotherm studies, PLoS One, 14 (2019) e0216878, https://doi.org/10.1371/journal.pone.0216878.
[11] Z. Kovacova, S. Demcak, M. Balintova, Removal of copper from water solutions by adsorption on spruce sawdust, Proceedings, 16 (2019) 52, doi: 10.3390/proceedings2019016052.
[12] V. Prajaputra, Z. Abidin, W. Widiatmaka, Methylene blue removal using developed material from volcanic ash soils, Int. J. Sci. Technol. Res., 8 (2019) 706–709.
[13] Q. Zhang, Y. Zhang, J. Chen, Q. Liu, Hierarchical structure kaolinite nanospheres with remarkably enhanced adsorption properties for Methylene blue, Nanoscale Res. Lett., 14 (2019) 104, https://doi.org/10.1186/s11671-019-2934-x.
[14] S. Lubis, Sheilatin, V. Prajaputra, N.S. Sepia, Preparation and characterization of titania/bentonite composite application on the degradation of naphthol blue black dye, Res. J. Chem. Environ., 22 (2018) 48–53.
[15] K. Jahangiri, N. Yousefi, S.K. Ghadiri, R. Fekri, A. Bagheri, S.S. Talebi, Enhancement adsorption of hexavalent chromium onto modified fly ash from aqueous solution; optimization; isotherm, kinetic and thermodynamic study, J. Dispersion Sci. Technol., 40 (2019) 1147–1158.
[16] M. Shafiee, M.A. Abedi, S. Abbasizadeh, R.K. Sheshdeh, S.E. Mousavi, S. Shohani, Effect of zeolite hydroxyl active site distribution on adsorption of Pb(II) and Ni(II) pollutants from water system by polymeric nanofibers, Sep. Sci. Technol., 55 (2019) 1–18.
[17] Y. Zheng, X. Li, P.K. Dutta, Exploitation of unique properties of zeolites in the development of gas sensors, Sensors (Basel), 12 (2012) 5170–5194.
[18] S.M.J. Mirzaei, M. Heidarpour, S.H. Tabatabaei, P. Najafi, S.E. Hashemi, Immobilization of leachate's heavy metals using soil-zeolite column, Int. J. Recyl. Org. Waste Agric., 2 (2013) 20, https://doi.org/10.1186/2251-7715-2-20.

[19] N. Martín, P.N.R. Vennestrøm, J.R. Thøgersen, M. Moliner, A. Corma, Fe-containing zeolites for NH_3–SCR of NO_x: effect of structure, synthesis procedure, and chemical composition on catalytic performance and stability, Chem. Eur. J., 23 (2017) 13404–13414.
[20] N.L.M. Tri, P.Q. Thang, L.V. Tan, P.T. Huong, J. Kim, N.M. Viet, N.M. Phuong, T.M.A. Tahtamouni, Removal of phenolic compounds from wastewaters by using synthesized Fe-nano zeolite, J. Water Process Eng., 33 (2020) 101070, https://doi.org/10.1016/j.jwpe.2019.101070.
[21] G.D. Pirngruber, P.K. Roy, R. Prins, On determining the nuclearity of iron sites in Fe-ZSM-5—a critical evaluation, Phys. Chem. Chem. Phys., 8 (2006) 3939–3950.
[22] R. Gonzalez-Olmos, F.-D. Kopinke, K. Mackenzie, A. Georgi, Hydrophobic Fe-zeolites for removal of MTBE from water by combination of adsorption and oxidation, Environ. Sci. Technol., 47 (2013) 2353–2360.
[23] B. Ersoy, A. Sariisik, S. Dikmen, G. Sariisik, Characterisationof acidic pumice and determination of its electrokinetic properties in water, Powder Technol. 197 (2010) 129–135.
[24] M.R. Samarghandi, M. Zarrabi, A. Amrane, M.M. Soori, M.N. Sepehr, Removal of acid black dye by pumice stone as a low cost adsorbent: kinetic, thermodynamic and equilibrium studies, Environ. Eng. Manage. J., 12 (2012) 2137–2147.
[25] M.R. Panuccio, A. Sorgonà, M. Rizzo, G. Cacco, Cadmium adsorption on vermiculite, zeolite and pumice: batch experimental studies, J. Environ. Manage., 90 (2009) 364–374.
[26] M.N. Sepehr, A. Amrane, K.A. Karimaian, M. Zarrabi, H.R. Ghaffari, Potential of waste pumice and surface modified pumice for hexavalent chromium removal: characterization, equilibrium, thermodynamic and kinetic study, J. Taiwan Inst. Chem. Eng., 45 (2014) 635–647.
[27] V. Prajaputra, Z. Abidin, Widiatmaka, D.T. Suryaningtyas, H. Rizal, Characterization of Na-P1 zeolite synthesized from pumice as low-cost materials and its ability for Methylene blue adsorption, IOP Conf. Ser.: Earth Environ. Sci., 399 (2019) 012014.
[28] M. Shaban, M.R. Abukhadra, A.A.P. Khan, B.M. Jibali, Removal of Congo red, Methylene blue and Cr(VI) ions from water using natural serpentine, J. Taiwan Inst. Chem. Eng., 82 (2018) 102–116.
[29] X. Li, W. Yang, Q. Zou, Y. Zuo, Investigation on microstructure, composition, and cytocompatibility of natural pumice for potential biomedical application, Tissue Eng. Part C Methods, 16 (2009) 427–434.
[30] E.A. Hildebrando, C.G.B. Andrade, C.A.F. da Rocha Junior, R. Angélica, F. Valenzuela-Díaz, R. Neves, Synthesis and characterization of zeolite NaP using kaolin waste as a source of silicon and aluminum, Mater. Res., 17 (2014) 174–179.
[31] A.I.M. Ismail, O.I. El-Shafey, M.H.A. Amr, M.S. El-Maghraby, Pumice characteristics and their utilization on the synthesis of mesoporous minerals and on the removal of heavy metals, Int. Scholarly Res. Notices, 2014 (2014) 259379, https://doi.org/10.1155/2014/259379.
[32] G. Asgari, B. Roshani, G. Ghanizadeh, The investigation of kinetic and isotherm of fluoride adsorption onto functionalize pumice stone, J. Hazard. Mater., 217 (2012) 123–132.
[33] A. Günay, E. Arslankaya, İ. Tosun, Lead removal from aqueous solution by natural and pretreated clinoptilolite: adsorption equilibrium and kinetics, J. Hazard. Mater., 146 (2007) 362–371.
[34] A. Nimibofa, A. Ekubo, W. Donbebe, E. Dikio, Adsorption of congo red by Ni/Al-CO_3: equilibrium, thermodynamic and kinetic studies, Orient. J. Chem., 31 (2015) 1307–1318.
[35] A.M.M. Vargas, A.L. Cazetta, M.H. Kunita, T.L. Silva, V.C. Almeida, Adsorption of Methylene blue on activated carbon produced from flamboyant pods (*Delonix regia*): study of adsorption isotherms and kinetic models, Chem. Eng. J., 168 (2011) 722–730.
[36] Q. Wang, S. Tian, P. Ning, Degradation mechanism of Methylene blue in a heterogeneous Fenton-like reaction catalyzed by ferrocene, Ind. Eng. Chem. Res., 53 (2014) 643–649.
[37] F. Jafari-zare, A. Habibi-yangjeh, Competitive adsorption of Methylene blue and rhodamine B on natural zeolite: thermodynamic and kinetic studies, Chin. J. Chem. Eng., 28 (2010) 349–356.
[38] P. Janoš, H. Buchtová, M. Rýznarová, Sorption of dyes from aqueous solutions onto fly ash, Water Res., 37 (2003) 4938–4944.
[39] C.D. Woolard, J. Strong, C.R. Erasmus, Evaluation of the use of modified coal ash as a potential sorbent for organic waste streams, Appl. Geochem., 17 (2002) 1159–1164.
[40] D. Ghosh, K.G. Bhattacharyya, Adsorption of Methylene blue on kaolinite, Appl. Clay Sci., 20 (2002) 295–300.